THE JOURNAL OF BIOLOGICAL CHEMISTRY VOL. 289, NO. 8, pp. 5340–5347, February 21, 2014

A Low-dose Arsenic-induced p53 Protein-mediated Metabolic Mechanism of Radiotherapy Protection*

Received for publication, October 30, 2013, and in revised form, January 2, 2014 Published, JBC Papers in Press, January 3, 2014, DOI 10.1074/jbc.M113.531020

Suthakar Ganapathy[‡], Shaowen Xiao[§1], Mei Yang[‡], Min Qi[§], Doo Eun Choi[‡], Chul S. Ha[§], John B. Little[‡], and Zhi-Min Yuan[‡2]

From the [‡]Department of Genetics and Complex Diseases, Harvard School of Public Health, Boston, Massachusetts 02115 and the [§]Department of Radiation Oncology, University of Texas Health Science Center at San Antonio, San Antonio, Texas 78229

Background: Radiotherapy protection depends on a selective protection of normal tissues but not tumors.
Results: We demonstrate that low doses of arsenic induce a p53/HIF-1α-dependent metabolic reprogramming specific to normal cells, resulting in increased resistance to radiation toxicity.
Conclusion: p53-mediated metabolic reprogramming can be explored for normal tissue protection.
Significance: The use of low-dose arsenic for selective protection of normal tissues may have important therapeutic implications.

Radiotherapy is the current frontline cancer treatment, but the resulting severe side effects often pose a significant threat to cancer patients, raising a pressing need for the development of effective strategies for radiotherapy protection. We exploited the distinct metabolic characteristics between normal and malignant cells for a metabolic mechanism of normal tissue protection. We showed that low doses of arsenic induce HIF-1α, which activates a metabolic shift from oxidative phosphorylation to glycolysis, resulting in increased cellular resistance to radiation. Of importance is that low-dose arsenic-induced HIF-1α requires functional p53, limiting the glycolytic shift to normal cells. Using tumor-bearing mice, we provide proof of principle for selective normal tissue protection against radiation injury.

Even with the growing development of targeted cancer therapies, radiation therapy remains an important cancer treatment modality. Ionizing radiation kills cells non-selectively via induction of DNA damage (1). Of great importance to an effective radiation treatment is to develop strategies able to preferentially sensitize cancer cells or desensitize normal tissues to irradiation. Many cellular processes, including metabolism, can modulate radiation sensitivity (2). In contrast with normal cells, which primarily use the mitochondrion oxidative phosphorylation pathway for energy production, malignant cells depend chiefly on aerobic glycolysis to support cell survival and proliferation (3). This distinct metabolic characteristic of cancer and normal cells may represent an opportunity to develop novel strategies of selectively target cancer cells while sparing normal tissues.

Hypoxia-inducible factor 1(HIF-1)[3] is a master transcription factor that controls the expression of a host of genes that mediate many cellular processes, including metabolism (4, 5). HIF-1 is a heterodimer consisting of O_2-sensitive HIF-1α and a constitutively expressed HIF-1β subunit. Under normoxia condition, HIF-1α is degraded rapidly, but hypoxia leads to stabilization and accumulation of the HIF-1α protein (4, 5). However, under certain normoxia conditions, HIF-1α expression can also be increased. For instance, the NFκB pathway stimulates transcription of *HIF-1α* (6, 7), the PI3K/AKT/mammalian target of rapamycin pathway promotes HIF-1α mRNA translation (5), and reactive oxygen species inhibit HIF-1α degradation (8, 9). Upon induction, HIF-1α stimulates the transcription of genes encoding glucose transporters and enzymes of glycolysis and the pentose phosphate pathway (2, 3). Consistent with the generally increased activity of the NFκB and PI3K/AKT/mammalian target of rapamycin pathways in malignant cells, HIF-1α is frequently elevated, which is, at least in part, responsible for the glycolytic phenotype of cancer cells (4, 5).

In this study, we exploited the different metabolic feature between cancer and normal cells for a strategy of selective normal tissue protection. We show that treatment with low doses of arsenic induced HIF-1α preferentially in normal cells, resulting in a metabolic switch from oxidative phosphorylation to glycolysis and increased radiation resistance. Using tumor-bearing mice, we obtained proof of principle for a selective normal tissue protection against radiation injury.

EXPERIMENTAL PROCEDURES

Reagents—All chemicals were purchased from Sigma-Aldrich (St. Louis, MO).

Cell Culture—Human fibroblasts (GM08680) and human B-lymphocytes (GM03798) were purchased from Coriell, (Camden, NJ). A549 human lung cancer cells were purchased from the ATCC. Human B-lymphocytes and A549 cells were maintained in RPMI 1640 medium (Corning Cellgro). Human

* This work was supported, in whole or in part, by NCI, National Institutes of Health Grants 2 R01CA085679, RO1CA167814, and RO1CA125144. This work was also supported by the Morningside Foundation and by Department of Energy Grants DOE 110976 and 65089.
[1] Present address: Beijing University Cancer Hospital, Beijing 100142, China.
[2] To whom correspondence should be addressed: Dept. of Genetics and Complex Diseases, Harvard School of Public Health, SPH-I, Rm. 509, 655 Huntington Ave., Boston, MA 02115. Tel.: 617-432-2139; Fax: 617-432-5236; E-mail: zyuan@hsph.harvard.edu.

[3] The abbreviations used are: HIF, hypoxia-inducible factor; Gy, gray; 2-DG, 2-deoxyglucose; LDH-A, lactate dehydrogenase-A; IR, ionizing radiation.

fibroblasts were maintained in DMEM (Corning Cellgro). All media were supplemented with 10% fetal bovine serum and 1% penicillin/streptomycin/gentamycin (Invitrogen) in a humidified atmosphere at 37 °C and 5% O_2, 5% CO_2.

Immunofluorescence—For immunofluorescence, human fibroblasts were fixed, permeabilized, and blocked, followed by incubation with primary antibodies overnight. Antibodies were from Cell Signaling Technology (phospho-Ser-139 H2AX), Novus Biologicals (HIF-1α), and Invitrogen (DAPI, rabbit Alexa Flour 488, and mouse Alexa Flour 594). A Nikon TE2000 microscope and Nikon Instruments Software elements software were used for imaging.

SiRNA Transfection—siRNAs were purchased from Sigma-Aldrich. Multiple sequences of siRNAs were used for p53, lactate dehydrogenase-A (LDH-A), HIF-1α, and NFκB. siRNAs were reverse-transfected using Lipofectamine RNAiMAX (Invitrogen) according to the instructions of the manufacturer. siGL2 was used as the negative control.

RNA Isolation and Quantitative RT-PCR—Total RNA was isolated using TRIzol reagent (Invitrogen) according to the instructions of the manufacturer. 1 μg of total RNA was used to make cDNA (iScript cDNA synthesis kit, Bio-Rad), following the instructions of the manufacturer, which was subsequently used for the amplification by quantitative RT-PCR using Applied Biosystem StepOnePlus in the presence of SYBR Green JumpStart (Sigma-Aldrich). Ribosomal 18 S RNA was used as the endogenous normalization control. The n-fold change in mRNA expression was determined on the basis of the ΔΔCt value. All assays were performed in triplicate.

Immunoblotting—Cells were washed with ice-cold phosphate-buffered saline and then lysed using lysis buffer (20 mM Tris-HCl (pH 7.5), 5 mM EDTA, 150 mM NaCl, 1% Nonidet P-40, 1 mM Na3VO4, 1 mM PMSF, and 0.1% protease inhibitor) for 45 min on ice. The cell extracts were centrifuged at 12,000 rpm for 15 min at 4 °C. Equal amounts of cell lysates were separated by SDS-PAGE. The separated proteins were transferred to a nitrocellulose membrane and immunoblotted using the indicated antibodies. Antibodies were from BD Biosciences (HIF-1α), Cell Signaling Technology (HK-2, Glc-6-PD, PFK-2, HK-1, ENO-2, P-AKT[T308], P-ERK[T202/Y204], and P-P65-[S536]), Abcam (Glut-1), and Sigma-Aldrich (β-actin). The protein bands were developed using HRP-conjugated secondary antibodies with ECL reagent.

Metabolic Flux Analysis—Flux studies were performed according to a published protocol (18) by treating human fibroblast cells with arsenic for a 12-h period and washed thoroughly with glucose-free medium and incubated the cells with medium containing 10 mM 1:1 mixture of D-[1,2-^{13}C]glucose and unlabeled D-glucose for 15 min. Metabolites were extracted on dry ice with 80% methanol. The metabolites were dried under nitrogen and resuspended in 20 μl of water for LC-MS analysis.

Apoptosis Assay—Apoptosis were determined by FACS analysis using an annexin V-FITC apoptosis detection kit (BioVision). Human B-lymphocytes were washed with phosphate-buffered saline, and the cell pellet was resuspended with 500 μl of 1× binding buffer. Annexin V-FITC (5 μl) and propidium iodide (50 mg/ml) were added and incubated at room temperature for 5 min in the dark. Samples were analyzed for apoptosis using flow cytometry (FACSCalibur, BD Biosciences).

Animal Experiments—All the procedures on animals were conducted in accordance with the guidelines for the Institutional Animal Care and Use Committee at the University of Texas Health Science Center at San Antonio, Texas. Mice used in this study were housed under pathogen-free conditions and maintained in a 12-h light/12-h dark cycle with food and water supplied *ad libitum*. A549 cells (3×10^6 cells mixed with Matrigel, BD Biosciences) in a final volume of 100 μl were injected into the flank region of 4- to 6-week-old BALB/$c^{nu/nu}$ mice (Harlan Laboratories). When tumors reached 0.1 cm, mice were randomized into four groups for treatment. Group I was the control, group II was treated with arsenic (0.4 mg/kg body weight for 3 days), group III was treated with x-rays (2 Gy/min for 5 days), and group IV treated with arsenic (0.4 mg/kg body weight for 3 days) + x-rays (2 Gy/min for 5 days).

Histological Analysis—Tissues were fixed with 10% formalin, embedded in paraffin, and sectioned. Hematoxylin and eosin staining was performed according to standard procedures.

Statistical Analysis—*In vitro* experiments were repeated at least three times. Two-way analysis of variance was used for the statistical calculation. Mann-Whitney *U* test was used for comparisons between different groups.

RESULTS

We recently reported that treatment with low doses of arsenic induced glycolysis in cells and mice (10). However, the underlying molecular mechanism remained incompletely understood. Given the well established role for HIF-1α in control of cellular metabolism (4, 5), we explored a potential involvement of this transcription factor in arsenic-induced metabolic change. Indeed, there was a marked induction of HIF-1α by low-dose arsenic treatment, as indicated by immunostaining showing a robust increase in the HIF-1α protein level in 0.1 μM arsenic-treated human fibroblasts (Fig. 1*A*). Measurement of the transcript revealed that the arsenic-induced increase in HIF-1α occurred at the mRNA level (Fig. 1*B*). A dose course experiment indicated that the induction of HIF-1α was specific to low doses of arsenic, specifically within the dose range of 0.05–0.5 μM (Fig. 1*C*). We further determined arsenic-induced HIF-1α activity by measuring the expression of GLUT-1, a target gene of HIF-1α. Treatment of fibroblasts with arsenic resulted in an increase in the GLUT-1 transcript with a pattern analogous to that of HIF-1α, confirming the induction of HIF-1α activity (Fig. 1*D*). A time course study was performed to examine the kinetics of HIF-1α induction by treatment with 100 nM arsenic. The result indicated that the arsenic-induced increase of HIF-1α was detectable 8 h after the treatment, reached a maximum at 12 h, and lasted over 24 h (Fig. 1*E*).

We went on to investigate the mechanism by which *HIF-1α* was induced by low-dose arsenic. Multiple cellular signaling pathways, including Akt and NFκB, have been implicated in the regulation of HIF-1α 5–7. We tested the potential contribution of these pathways by using specific inhibitors. The results of Western blot analyses indicated that inhibition of NFκB, but not Akt and Erk, blocked low-dose arsenic-induced HIF-1α

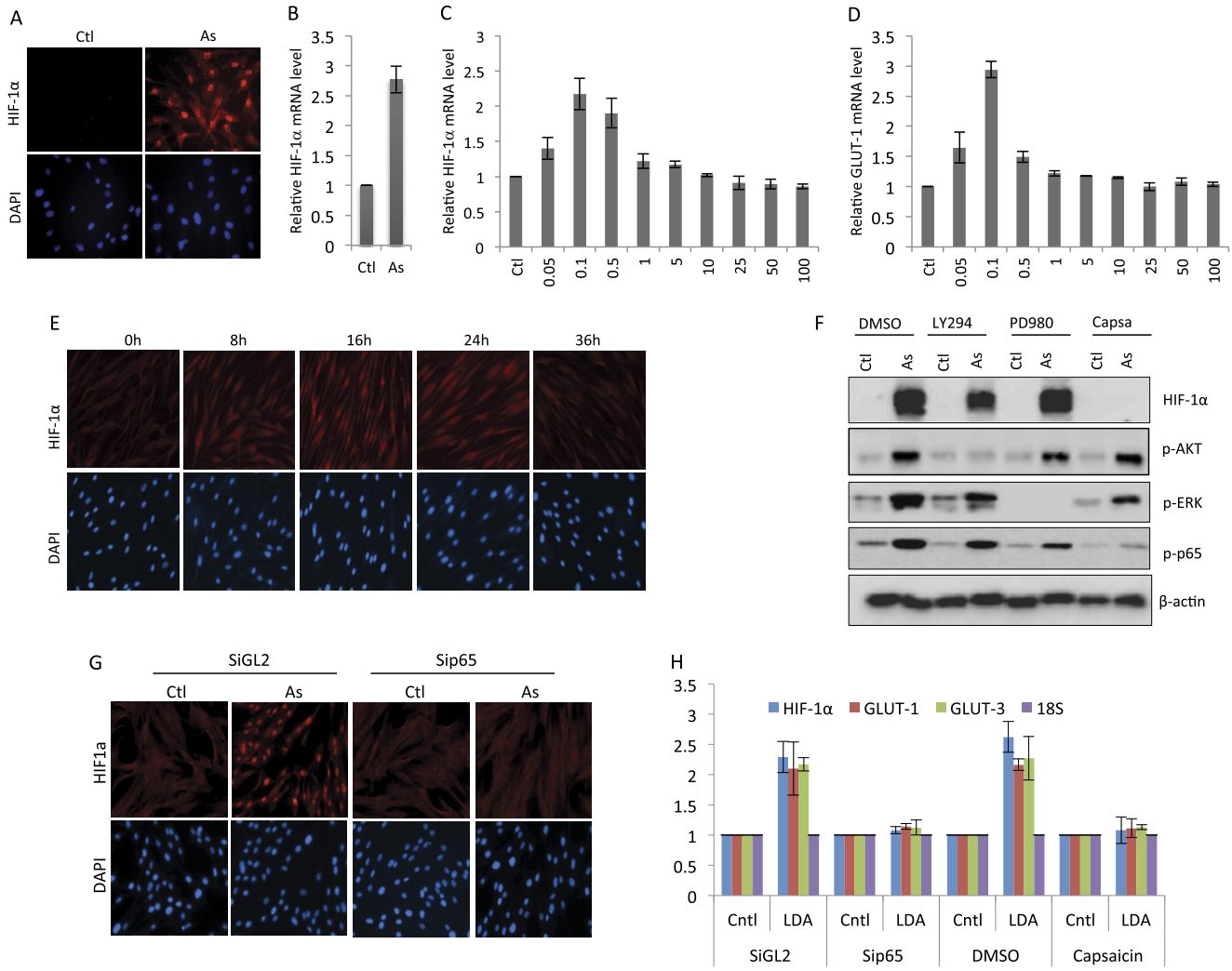

FIGURE 1. **Low doses of arsenic induce HIF-1α in an NFκB-dependent manner.** Human fibroblasts were treated with sodium arsenite (*As*) (100 nM) for 12 h. The cells were harvested for HIF-1α immunostaining (*A*) or analysis of the HIF-1α transcript (*B*) (*Ctl*, control). Human fibroblasts were treated with the indicated doses of sodium arsenite. The cells were harvested 12 h later and analyzed for the levels of HIF-1α transcript (*C*) or GLUT-1 transcript (*D*). Data are mean ± S.D. from three independent experiments. *F*, human fibroblasts were pretreated with dimethyl sulfoxide (*DMSO*), LY294002 (25 μM) (*LY294*), PD98049 (25 μM) (PD980), or capsaicin (3 μM) (*Capsa*) for 1 h. The cells were then treated with either solvent or 100 nM arsenic and harvested 12 h later for Western blot analysis using the indicated antibodies. *G*, human fibroblasts were transfected with either control RNAi (*siGL2*) or sip65. The cells were subjected to treatment with arsenic (100 nM) 48 h post-transfection. The cells were harvested 12 h later for HIF-1α immunostaining. *H*, human fibroblasts were transfected with either control RNAi or sip65 for 48 h or pretreated with dimethyl sulfoxide or capsaicin (3 μM) for 1 h. The cells were treated with either solvent (*Cntl*) or 100 nM arsenic (low dose arsenic, *LDA*). The cells were harvested 12 h later and analyzed for the levels of HIF-1α, GLUT-1, or GLUT-3 transcript. Data are mean ± S.D. from three independent experiments. *E*, human fibroblasts were treated with sodium arsenite for the indicated time periods, and the cells were immunostained for HIF-1α.

(Fig. 1*F*). To complement the data derived from the use of inhibitors, we employed an RNAi-mediated knockdown method. Knockdown of p65 indeed resulted in diminished HIF-1α induction, as shown by immunostaining (Fig. 1*G*). We also measured the transcripts level to validate the effect of NFκB inhibition on HIF-1α expression. Both sip65 and the inhibitor effectively blocked the induction of HIF-1α mRNA by low-dose arsenic (Fig. 1*H*). The transcripts of GLUT-3 and GLUT-1, the target genes of NFκB and HIF-1α, respectively, were monitored to reflect the transcriptional activity of NFκB and HIF-1α (Fig. 1*H*). Together, the results demonstrate an induction of HIF-1α specific to low-dose arsenic via an NF-κB-dependent mechanism.

Given that HIF-1α can regulate the expression of multiple metabolic enzymes (4, 5), the increased HIF-1α level would predict an altered expression of metabolic genes in arsenic-treated cells. We tested this prediction by measuring the expression of key enzymes in the metabolic pathways. The result indicates that the treatment of cells with low-dose arsenic induced a number of glycolytic genes (Fig. 2*A*, *left panel*). Of interest is the observation that the increase in glycolytic genes was associated with a decrease in TCA cycle genes (Fig. 2*A*, *right panel*). Increased levels of these metabolic enzymes by low-dose arsenic were also observed at the protein level (Fig. 2*B*). The data suggest a metabolic shift from oxidative phosphorylation to glycolysis, which is in line with the HIF-1α activity that stimulates the glycolytic genes while suppressing the TCA cycle genes (5, 11, 12). To determine whether HIF-1α was responsible for mediating the low-dose arsenic-induced alteration of metabolic gene expression, we performed RNAi-medi-

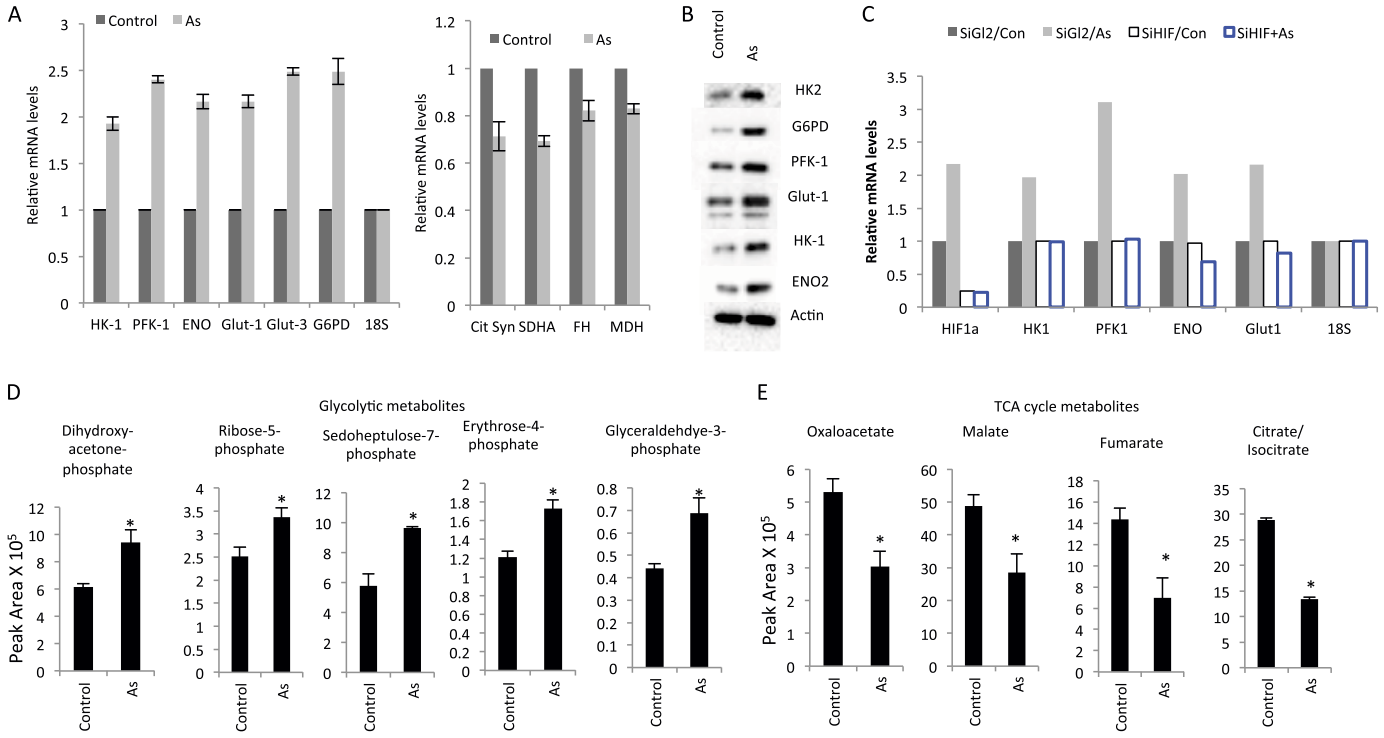

FIGURE 2. **Low-dose arsenic induces a metabolic shift.** *A*, human fibroblasts were treated with arsenic (*As*) (100 nM) for 12 h. mRNA was isolated, and the transcripts of the indicated genes were determined by quantitative RT-PCR. Data are mean ± S.D. from three independent experiments. *B*, arsenic-treated (100 nM) fibroblasts were subjected to Western blot analysis using the indicated antibodies. *C*, human fibroblasts were transfected with either control RNAi (*siGL2*) or siHIF-1α. The cells were subjected to treatment with arsenic (100 nM) 48 h post-transfection. The cells were harvested at 12 h later for analysis of the indicated transcripts. *Con*, control. *D* and *E*, fibroblasts were treated with arsenic (100 nM) for 12 h and incubated with D-[1,2-^{13}C]glucose for 15 min prior to metabolite extraction and targeted LC-MS/MS analysis. The ratio of ^{13}C-labeled to unlabeled (^{12}C) metabolites was measured by LC-MS/MS and is presented as mean ± S.D. over three independent samples (*, $p < 0.05$).

ated knockdown of HIF-1α. The result indicates that arsenic-induced expression of glycolytic genes indeed depended on HIF-1α, as reflected by a markedly diminished arsenic-mediated induction of genes encoding the glucose transporter and glycolysis in the HIF-1α-depleted cells (Fig. 2*C*). Together, the results indicate that low doses of arsenic induce HIF-1α, resulting in elevated expression of glucose transporters and metabolic genes.

To more accurately characterize the low-dose arsenic-induced metabolic response, we performed a stable isotope flux analysis using LC/MS-based metabolomics following the labeling of cells with D-[1,2-^{13}C]glucose. The results indicated a clear increase of ^{13}C-labeled glycolytic intermediates in arsenic-treated cells (Fig. 2*D*), which was associated with a concomitant decrease of TCA cycle metabolites (Fig. 2*E*), consistent with a metabolic switch from oxidative phosphorylation to glycolysis.

As a process fundamental to cellular functions, cellular metabolism will likely affect the cellular response to radiation (2, 3). We asked whether arsenic-induced HIF1α might modulate cellular radiation sensitivity and performed a clonogenic survival assay. Pretreatment of human fibroblasts with 100 nM sodium arsenite substantially reduced cell killing induced by a 4-Gy dose (Fig. 3*A*). The low-dose arsenic-induced resistance was also evident at the level of DNA damage, measured with the surrogate marker γH2AX (13) (Fig. 3*B*). Quantitative analysis of γH2AX focus-positive cells indicated a marked increase in radiation resistance by arsenic pretreatment (Fig. 3*C*). We then examined the role of HIF-1α in arsenic-induced radiation resistance by using siRNA-mediated knockdown of HIF-1α expression. Low-dose arsenic-induced resistance to radiation was almost completely diminished in HIF-1α-depleted cells, indicating an indispensable role of this transcription factor (Fig. 3*D*). Measurement of radiation-induced γH2AX further supported a HIF-1α-dependent radiation resistance (Fig. 3*E*). To determine whether HIF-1α-dependent protection was mediated by glucose metabolism, we inhibited glycolysis by either limiting the glucose supply or using 2-deoxyglucose (2-DG), an inhibitor of glycolysis. The arsenic-induced resistance was almost completely lost when glucose levels were reduced to 2 mM or cells were treated with 2-DG (Fig. 3*F*). The importance of glucose uptake and glycolysis in low-dose arsenic-induced resistance was also observed in human lymphocytes (Fig. 3*H*), indicating that the effect is not cell type-specific. To complement the use of glucose restriction and 2-DG, we employed RNAi to knock down the expression of LDH-A, an enzyme critical to glycolysis (2, 3). A similar effect to that of 2-DG was seen on the levels of γH2AX foci as well as cell survival, demonstrating a loss of induced resistance (Fig. 3*G*). Together, the data demonstrate that pretreatment of human fibroblasts and lymphocytes with low-dose arsenic was associated with an increase in radiation resistance and that the protective effect of arsenic was mediated by HIF-1α-dependent induction of glycolysis.

We showed previously that suppression of functional p53 was a prerequisite for low doses of arsenic-induced glycolysis

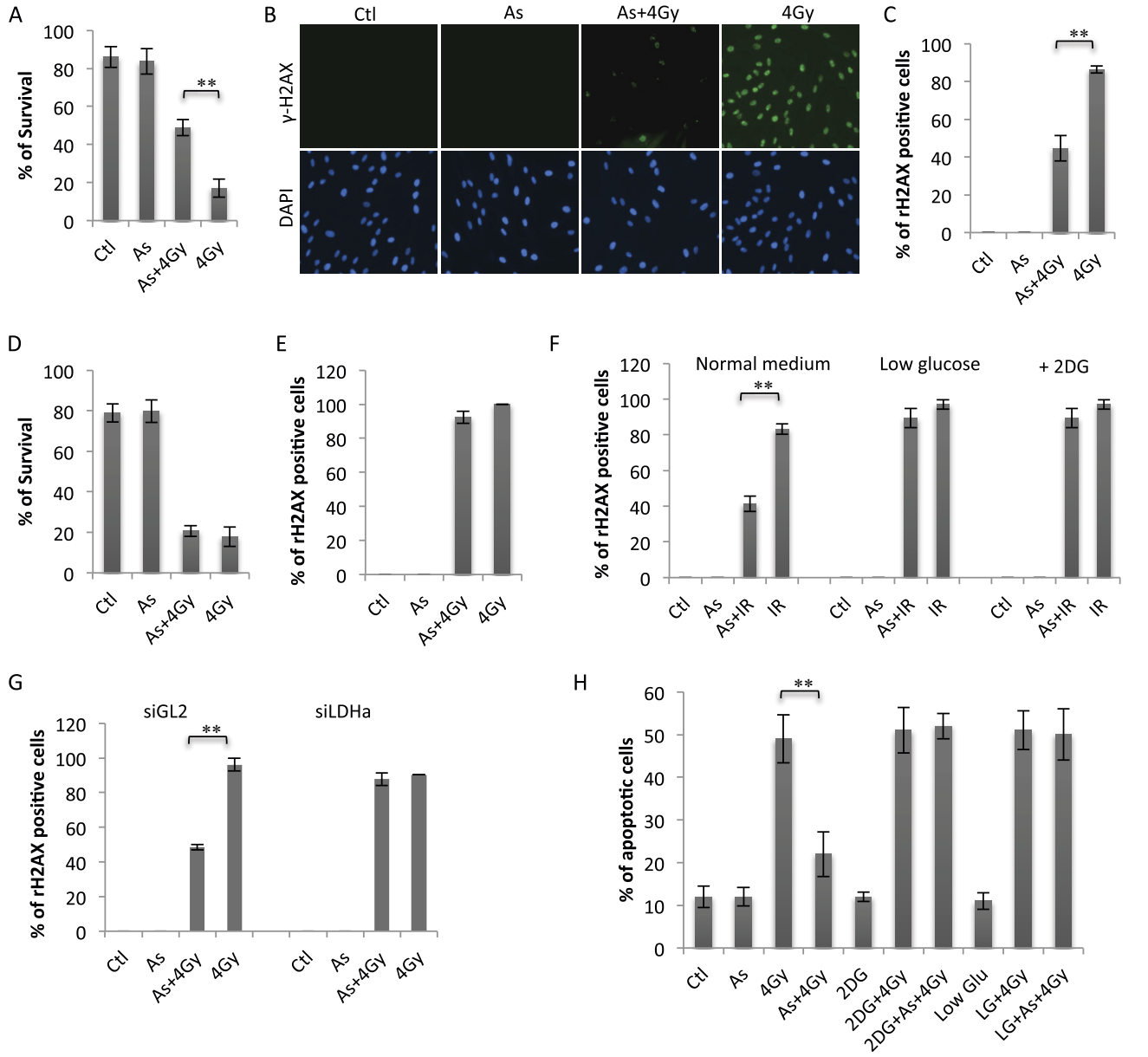

FIGURE 3. **Low-dose arsenic induces radiation resistance via induction of HIF-1α-dependent glycolysis.** *A*, human fibroblasts were pretreated with or without arsenic (*As*) (100 nM) for 12 h, followed by 4-Gy irradiation. The cells were also subjected to colony survival assays. Data are mean ± S.D. from three independent experiments. **, $p < 0.01$. *Ctl*, control. *B*, fibroblasts were treated as indicated. The cells were harvested 1 h after irradiation and subjected to γH2AX immunostaining. *C*, quantification of γH2AX-positive cells shown in *B*. *Error bars* represent mean ± S.D. of three independent experiments (~100 cells/sample). **, $p < 0.01$. *D*, human fibroblasts were transfected with either control RNAi (*siGL2*) or siHIF-1α. 48 h post-transfection, the cells were pretreated with arsenic (100 nM) for 12 h and then irradiated at 4 Gy. The cells were analyzed via colony survival assay. Data are mean ± S.D. from three independent experiments. *E*, siGL2 or siHIF-1α-expressing cells were pretreated with arsenic (100 nM), followed by 4-Gy irradiation as in *E*. The cells were analyzed for γH2AX 1 h after IR treatment. The numbers of γH2AX-positive cells are presented as mean ± S.D. of three independent experiments (~100 cells/sample). **, $p < 0.01$. *F*, human fibroblasts cultured in normal medium or low-glucose (2 mM) medium were pretreated with arsenic (100 nM) or left untreated, followed after 12 h by 0- or 4.0-Gy treatment. Fibroblasts cultured in normal medium were treated with 2-DG (5 mM) 2 h before 4-Gy treatment. The cells were fixed 1 h post-4-Gy treatment and analyzed as in *E*. *G*, siGL2- or siLDH-A-expressing cells were treated and analyzed as in *E*. *H*, human lymphocytes were treated as in F and analyzed for the percentage of apoptosis. Bars represent mean ± S.D. of three independent experiments, **, $p < 0.01$.

(10). Given that HIF-1α is required for low-dose arsenic-induced glycolysis, we asked whether p53 was similarly involved in the regulation of HIF-1α. Human fibroblasts were pretreated with a low dose of Nutlin-3a, a p53-specific activator (14). Interestingly, under the condition of mild p53 activation, low-dose arsenic-induced HIF-1α was blocked completely (Fig. 4*A*, *As versus Nutlin 3a+As*), suggesting that p53 inhibition is necessary for HIF-1α induction. Correlated with the HIF-1α was the cellular sensitivity. In Nutlin 3a-treated cells, arsenic was no longer able to induce radiation resistance. The levels of irradiation-induced γH2AX were comparable in the presence or absence of arsenic (Fig. 4*B*). We further tested the p53 requirement by depleting p53 expression with siRNA. Indeed, down-regulation of p53 nearly eliminated the difference of cellular sensitivity to irradiation between arsenic-treated and untreated cells (Fig. 4*C*).

The requirement of functional p53 in the HIF-1α response raised the possibility that cancer cells with wild-type p53 may

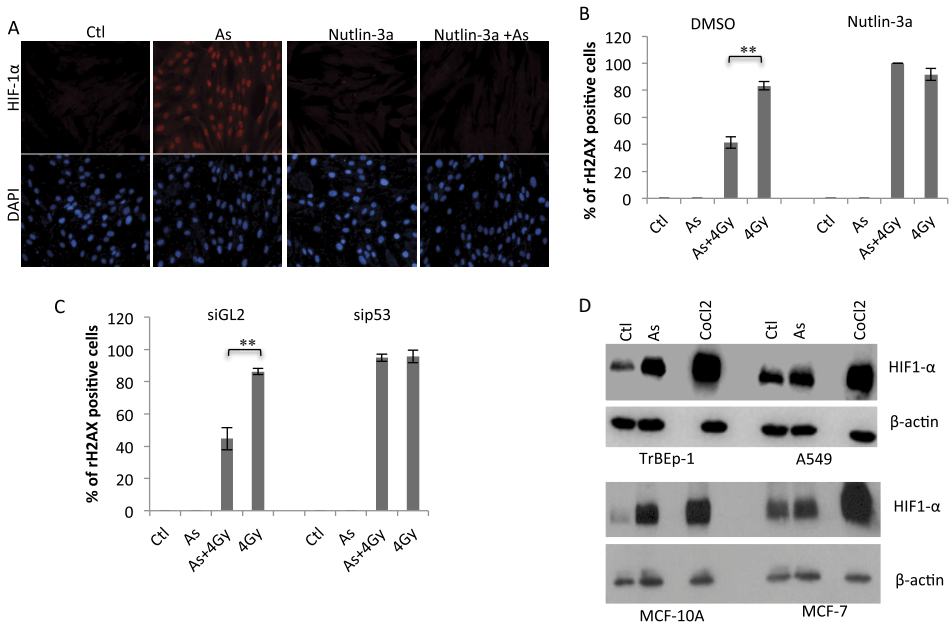

FIGURE 4. **Functional p53 is required for mediating low-dose arsenic-induced HIF-1α-dependent radiation resistance.** *A*, fibroblasts were pretreated with or without Nutlin 3A (10 μM) for 2 h prior to being treated with arsenic (*As*). The cells were harvested 12 h after arsenic treatment and subjected to HIF-1α immunostaining. *Ctl*, control. *B*, fibroblasts were treated with or without Nutlin 3A 2 h before being treated with arsenic, followed by irradiation. The cells were analyzed by γH2AX immunostaining and quantified as described in Fig. 3*C*. *DMSO*, dimethyl sulfoxide. Bars represent mean ± S.D. of three independent experiments (~100 cells/sample), **, $p < 0.01$. *C*, siGL2- or sip53-expressing cells were pretreated with arsenic (100 nM) or left untreated, followed after 12 h by 0- or 4.0-Gy treatment. The cells were fixed 1 h post-4-Gy treatment and analyzed as in Fig. 3*C*. Bars represent mean ± S.D. of three independent experiments (100 cells/sample), **, $p < 0.01$. *D*, human non-transformed lung epithelial cells (*TrBEp-1*) or lung carcinoma cells (*A549*) were treated with arsenic (100 nM) or $CoCl_2$ (100 μM) for 12 h. The cells were analyzed by Western blot analysis using the indicated antibodies. MCF-10A/MCF-7 cells were included as control.

also be protected by low-dose arsenic. We tested this possibility with a human lung carcinoma cell line, A549, that expresses wild-type p53 (15). Interestingly, treatment of A549 cells with 100 nM arsenic was associated with little change of HIF-1α, whereas this lung carcinoma cell line responded to $CoCl_2$ with a robust HIF-1α induction (Fig. 4*D*). When tested under the same experimental condition, TrBEp-1, a non-transformed lung epithelial cell line, displayed a marked induction of HIF1α in response to 100 nM arsenic as well as $CoCl_2$ treatment (Fig. 4*D*). The result suggests that low-dose arsenic-induced HIF-1α seemed to limit to non-transformed cells. This notion was validated with additional pair cell lines: MCF-10A/MCF-7.

Given that treatment of A549 cells with low-dose arsenic did not induce HIF-1α (Fig. 4*D*), we predict that this lung carcinoma cells would not be protected by low-dose arsenic treatment despite its wild-type p53 status. We tested this prediction with a mouse xenograft model implanted with A459 cells. Treatments were initiated when the tumor reached an average volume ~100 mm^3. The mice were pretreated with or without 0.4 mg/kg sodium arsenite for 3 days before being subjected to IR treatment. The tumor volume in the vehicle group continued to increase with time (Fig. 5*A*). Low-dose arsenic treatment did not have any detectable effect on tumor growth (Fig. 5*A*). IR treatment (total body irradiation) daily for 5 days resulted in marked tumor inhibition (Fig. 5*A*). Significantly, low-dose arsenic pretreatment showed little effect on IR-induced tumor suppression because IR-induced tumor regression is indistinguishable in mice that were pretreated with or without low-dose arsenic (Fig. 5*A*). There was little difference between male and female mice in response to the treatment with IR and arsenic (Fig. 5*A*). Thus, our data indicate that a brief pretreatment with low-dose arsenic did not detectably affect the efficacy of IR, at least in the human lung carcinoma xenograft mouse model.

To examine whether low-dose arsenic could alleviate IR-induced toxicity in these tumor-bearing mice, we monitored body weight changes. In contrast to control and low-dose arsenic-treated mice, IR-treated mice exhibited a significant reduction of body weight (Fig. 5*B*). This weight loss was most likely caused by IR toxicity and not the effect of tumors because we saw an almost complete recession of tumors in these animals (Fig. 5*A*). Remarkably, the IR-induced body weight loss was almost completely prevented in both male and female mice by arsenic pretreatment (Fig. 5*B*).

To corroborate the results of the body weight measurements, we assessed the effect of low-dose arsenic at the tissue level and observed a similar protection. Of note, arsenic treatment was associated with the induction of HIF-1α expression only in normal tissue (the small intestine) but not tumors, consistent with the *in vitro* data. IR-induced damage to the small intestine was markedly ameliorated by low-dose arsenic pretreatment (Fig. 5*C*). The protective effect of arsenic is also evident in bone marrow. Bone marrow cell exhaustion was clearly observed in IR-treated mice. However, this decrease of bone marrow cellularity was considerably alleviated in low-dose arsenic-pretreated mice (Fig. 5*D*). Collectively, the results demonstrate that a brief treatment with low-dose arsenic is associated with a marked protection of normal tissues without compromising the ability of IR to kill carcinoma cells.

DISCUSSION

Radiotherapy kills cancer cells primarily via induction of DNA damage, which, unfortunately, also causes normal tissue

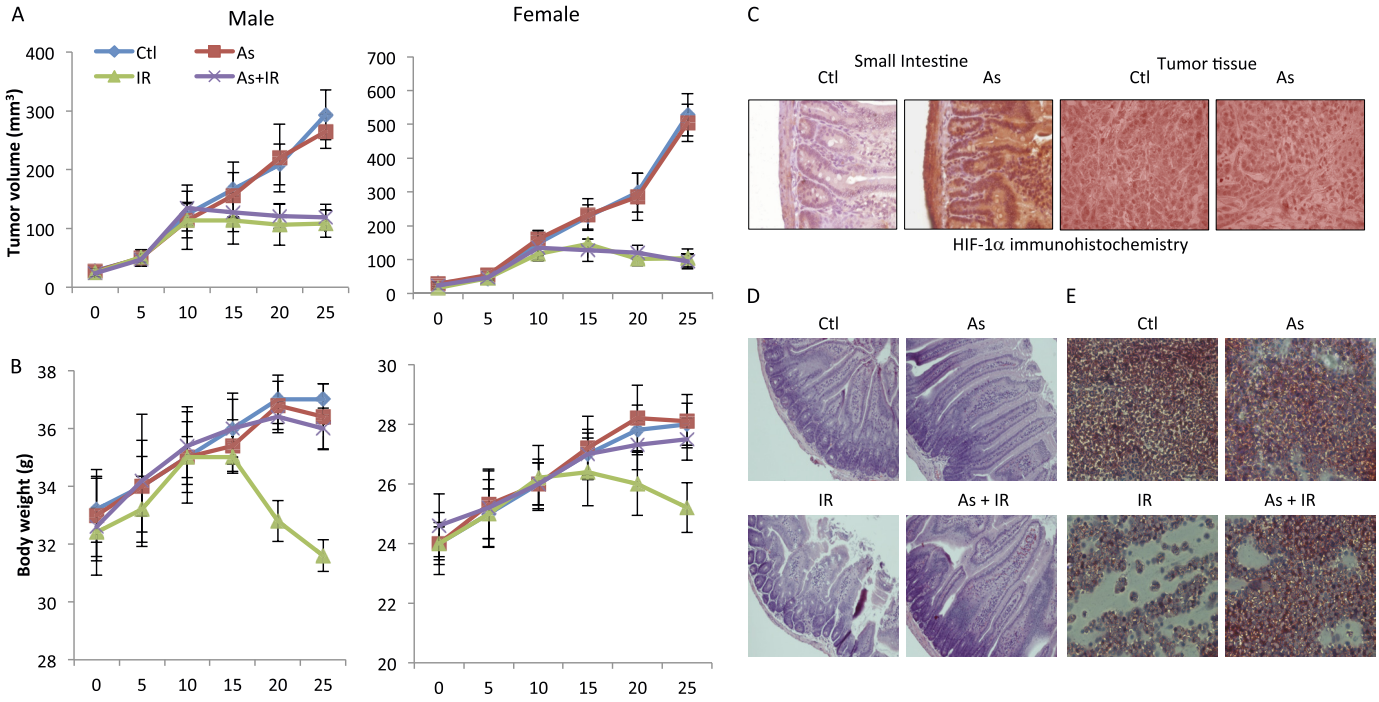

FIGURE 5. **Low-dose arsenic pretreatment alleviates normal tissue toxicity caused by total body irradiation of tumor-bearing mice.** Athymic nude mice (BALB/$c^{nu/nu}$, 4- to 6-week-old, sex-matched) were from Harlan Laboratories. The human lung carcinoma cell line A549 (cells as a 50% suspension in Matrigel) as 3 million cells/mouse in a final volume of 100 μl was injected subcutaneously into the right flank of BALB/c nude mice. When the average tumor volume reached about 100 mm^3, mice were randomized into the following groups: control (*Ctl*), arsenic (*As*) only, IR only, and arsenic and IR. For arsenic pretreatment, mice were treated with sodium arsenite (0.4 mg/kg body weight) for 3 days (days 0–3). Mice were then treated with total body irradiation at 2 Gy/day for 5 days. *A*, tumor volumes were measured every 5 days. The tumor volume was calculated using the equation volume = length × width × depth × 0.5236 mm^3. Two independent experiments were performed, and the tumor volumes are mean ± S.E. from a total of 10 mice/group. *B*, the body weight of the mice was monitored throughout the experiment as described in *A*. The numbers are mean ± S.D. from two independent experiments with a total of 10 mice/group. At the completion of the experiments, the mice were sacrificed by cervical decapitation. Tissue and tumor samples were harvested for histology experiments. *C*, the small intestine and tumor sections were stained for HIF-1α. H&E staining was performed. Representative images of H&E staining of the small intestine (*D*) and bone marrow (*E*) are shown.

injury. The major challenge for effective radiation therapy is the preservation of normal tissue while still accomplishing the effective killing of cancer cells. By exploiting the distinct metabolic characteristics between cancer and normal cells, we show that low doses of arsenic, through the induction of a metabolic reprogramming in normal cells, selectively protected normal tissues from radiation injury.

Arsenic trioxide is currently used to treat acute promyelocytic leukemia and is known as a cytotoxic agent (16). However, the arsenic dose we used in our *in vivo* experiments was ~30-fold lower than that in clinical use. When used in mice, such a low concentration of arsenic not only showed little toxicity but also did not have a detectable effect on the growth of cancer cells. The tumors derived from A549 cell implants developed with a comparable rate in mice treated with the vehicle or arsenic (Fig. 5*A*). Remarkably, although arsenic treatment did not interfere with the radiation-induced killing of cancer cells, it provided a considerable protection of animals from radiation toxicity. The results from the tumor-bearing mice provide proof of concept for the use of low-dose arsenic in radiotherapy protection.

We employed an integrated approach including biochemical, genetic, and metabolomics methods to gain mechanistic insights into arsenic-mediated normal tissue protection. We observed a robust up-regulation of cellular HIF-1α levels induced specifically by low doses of arsenic. Using a combination of pharmacological and genetic approaches, we showed that arsenic-induced HIF-1α seemed to be through, at least in part, NFκB-dependent transcriptional regulation, which is consistent with the fact that *HIF-1α* is a target gene of NFκB (6, 7) and the latter is stimulated by arsenic, as shown previously (10). Of significance is the finding that low-dose arsenic-induced HIF-1α is specific to non-transformed cells, which may constitute the basis of the observed selective protection of normal tissue. This distinct response of HIF-1α to low-dose arsenic in normal cells appeared to be mediated by functional p53, which served as the root of separating normal cells from malignant cells. The tumor suppressor p53 is universally inactivated in tumor cells by either gene mutation or deregulation (15). We showed previously that treatment of non-transformed cells with low-dose arsenic induces a transient and reversible p53 inhibition (10). Consistently, we found that p53 suppression seemed to be a prerequisite for low-dose arsenic to induce HIF-1α. Of note is that, despite its wild-type p53 status, A549 cells exhibited little HIF-1α induction in response to low-dose arsenic treatment, suggesting that p53 was not functioning normally in this lung carcinoma cell line, at least under our experimental conditions. The use of combined loss and gain of function approaches yielded solid evidence indicating a requirement of functional p53 in low-dose arsenic-induced HIF-1α. Studies have shown that p53 activity is critical in keep-

ing HIF-1α in check (17). The highly elevated basal level of HIF-1α in A549 cells is consistent with a defective p53 pathway.

It is intriguing that although functional p53 is necessary, its activity has to be kept in check for low-dose arsenic-induced radiation resistance. The necessity of restraint of p53 activity for arsenic-induced HIF-1α/glycolysis-dependent protection is in line with the functions of p53 in promoting cell death and inhibiting glycolysis (19). However, functional p53 with its activity at the basal level is necessary to maintain a cellular homeostatic state (15), which is crucial for a cell to respond to the relative low to moderate level of stress signals, such as low-dose arsenic treatment. Either a decrease or increase of the basal p53 activity would likely perturb cellular homeostasis, resulting in interference with the response of the cell to the modest stress signals. Clearly, further studies are necessary to gain a better understanding of this important question.

The contribution of HIF-1α to radiation resistance has been reported previously (17). We show that HIF-1α renders cells increasingly radiation-resistant via induction of glycolysis. As a master transcription factor in control of cellular metabolism, arsenic-induced HIF-1α stimulated the expression of genes encoding the glucose transporters and multiple glycolysis enzymes. Such an alteration of gene expression is expected to impact cellular metabolism. Indeed, the data from a metabolomics analysis revealed metabolic reprogramming from oxidative phosphorylation to glycolysis induced by low-dose arsenic treatment. Although aerobic glycolysis has been described as a unique metabolic feature of malignant cells (2, 3), our study indicates that glycolysis can also be induced in normal cells. Studies have shown that some metabolic intermediates or metabolites can serve as important cofactors for enzymes involved in chromatin modification as well as DNA repair (2, 3). The dependence of arsenic-induced reduction of rH2AX on the increased flux of glycolysis and the pentose phosphate pathway implicates a metabolic regulation of chromatin modification and DNA repair. Further studies are necessary to investigate how glycolytic metabolism renders cells resistant to radiation.

REFERENCES

1. Hall, E., and Giaccia, A. J. (2006) *Radiobiology for the Radiobiologist.* pp. 5–29, Lippincott Williams & Wilkins, Philadelphia, PA
2. Koppenol, W. H., Bounds, P. L., and Dang, C. V. (2011) Otto Warburg's contributions to current concepts of cancer metabolism. *Nat. Rev. Cancer* **11,** 325–337
3. Lunt, S. Y., and Vander Heiden, M. G. (2011) Aerobic glycolysis. Meeting the metabolic requirement of cell proliferation. *Annu. Rev. Cell Dev. Biol.* **27,** 441–464
4. Gordan, J. D., and Simon, M. C. (2007) Hypoxia-inducible factors, central regulators of the tumor phenotype. *Curr. Opin. Genet. Dev.* **17,** 71–77
5. Semenza, G. L. (2012) Hypoxia-inducible factors in physiology and medicine. *Cell* **148,** 399–408
6. van Uden, P., Kenneth, N. S., and Rocha, S. (2008) Regulation of hypoxia-inducible factor-1α by NF-κB. *Biochem. J.* **412,** 477–484
7. Rius, J., Guma, M., Schachtrup, C., Akassoglou, K., Zinkernagel, A. S., Nizet, V., Johnson, R. S., Haddad, G. G., and Karin, M. (2008) NF-κB links innate immunity to the hypoxic response through transcriptional regulation of HIF-1α. *Nature* **453,** 807–811
8. Pan, Y., Mansfield, K. D., Bertozzi, C. C., Rudenko, V., Chan, D. A., Giaccia, A. J., and Simon, M. C. (2007) Multiple factors affecting cellular redox status and energy metabolism modulate hypoxia-inducible factor prolyl hydroxylase activity *in vivo* and *in vitro*. *Mol. Cell. Biol.* **27,** 912–925
9. Finkel, T. (2012) Signal transduction by mitochondrial oxidants. *J. Biol. Chem.* **287,** 4434–4440
10. Ganapathy, S., Xiao, X., Seo, S., Lall, R., Yang, M., Xu, T., Su, H., Shadfan, M., Ha, C., and Yuan, Z. M. (2013) Low-dose arsenic induces chemotherapy protection via p53/NF-κB-mediated metabolic regulation. *Oncogene* 10.1038/onc.2013.81
11. Chan, S. Y., Zhang, Y. Y., Hemann, C., Mahoney, C. E., Zweier, J. L., and Loscalzo, J. (2009) MicroRNA-210 controls mitochondrial metabolism during hypoxia by repressing the iron-sulfur cluster assembly proteins ISCU1/2. *Cell Metab.* **10,** 273–284
12. Corn, P. G. (2008) Hypoxic regulation of miR-210. Shrinking targets expand HIF-1s influence. *Cancer Biol. Ther.* **7,** 265–267
13. Kastan, M. B., Onyekwere, O., Sidransky, D., Vogelstein, B., and Craig, R. W. (1991) Participation of p53 protein in the cellular response to DNA damage. *Cancer Res.* **51,** 6304–6311
14. Vassilev, L. T., Vu, B. T., Graves, B., Carvajal, D., Podlaski, F., Filipovic, Z., Kong, N., Kammlott, U., Lukacs, C., Klein, C., Fotouhi, N., Liu, E. A. (2004) *In vivo* activation of the p53 pathway by small-molecule antagonists of MDM2. *Science* **303,** 844–848
15. Vousden, K. H., and Prives, C. (2009) Blinded by the light, the growing complexity of p53. *Cell* **37,** 413–431
16. Powell, B. L. (2011) Arsenic trioxide in acute promyelocytic leukemia. Potion not poison. *Expert Rev. Anticancer Ther.* **11,** 1317–1319
17. Sermeus, A., and Michiels, C. (2011) Reciprocal influence of the p53 and the hypoxic pathways. *Cell Death Dis.* **26,** 164
18. Yuan, M., Breitkopf, S. B., Yang, X., and Asara, J. M. (2012) A positive/negative ion-switching, targeted mass spectrometry-based metabolomics platform for bodily fluids, cells, and fresh and fixed tissue. *Nat. Protoc.* **7,** 872–881
19. Vousden, K. H., and Ryan, K. M. (2009) p53 and metabolism. *Nat. Rev. Cancer* **9,** 691–700